Supporting Information for

Base-Pairing Energies of Proton-Bound Homodimers Determined by Guided Ion Beam Tandem Mass Spectrometry: Application to Cytosine and 5-Substituted Cytosines

Bo Yang, R. R. Wu, M. T. Rodgers*
Department of Chemistry, Wayne State University, Detroit, MI, 48202, USA

Data Handling: Measured ion intensities are converted to absolute cross sections using a Beer's law analysis as described previously.[1] Ion kinetic energies in the laboratory frame are converted to energies in the center-of-mass frame, E_{CM}, using the formula, $E_{CM} = E_{Lab}m/(m+M)$, where M and m are the masses of the $(5x\text{C})H^+(5x\text{C})$ complexes and neutral Xe atom, respectively. All energies reported below are in the center-of-mass frame unless otherwise noted. The absolute zero and distribution of ion kinetic energies are determined using the octopole ion guide as a retarding potential analyzer, as previously described.[1]

Because multiple ion-neutral collisions can influence the shape of the CID cross sections and the threshold regions are most sensitive to these effects, each CID cross section was measured twice at three nominal pressures (0.05, 0.075, and 0.10 mTorr). Date free from pressure effects are obtained by extrapolating to zero pressure of the Xe reactant, as described previously.[2] Therefore, the CID cross sections subjected to thermochemical analysis are ensured to be the result of single $(5x\text{C})H^+(5x\text{C})$–Xe collisions.

Thermochemical Analysis. The threshold regions of the measured CID cross sections are modeled using procedures developed elsewhere. an empirical threshold law, eq S1,

$$\sigma(E) = \sigma_0 \sum_i g_i (E + E_i - E_0)^n / E \qquad \text{(S1)}$$

where σ_0 is an energy independent scaling factor, E is the relative translational energy of the proton-bound homodimer and the Xe atom, E_0 is the threshold for reaction of the ground electronic and ro-vibrational state, and n is an adjustable parameter that describes the efficiency of kinetic to to internal energy transfer.[3] The summation is over the ro-vibrational states of the reactant ions, i, where E_i is the excitation energy of each state, and g_i is the population of those states (Σg_i=1).

The Beyer-Swinehart algorithm[4-6] is used to evaluate the density of the ro-vibrational states, i, and the relative populations of those states, g_i, are calculated as a Maxwell-Boltzman distribution at 298 K, the internal temperature of the reactant proton-bound homodimer. Vibrational frequencies and rotational constants of the reactant complexes are determined from theoretical calculations, as described in the Computation Details section. To account for the inaccuracies in the computed frequencies, we have increased and decreased the prescaled frequencies by 10%.

Another consideration in the analysis of CID thresholds is whether dissociation of the activated proton-bound homodimer occurs within the time frame of the experiment (~10^{-4} s). If the lifetime of the activated complex exceeds this time frame, the apparent thresholds shift to higher energies, resulting in a kinetic shift. Therefore, the data for all five proton-bound homodimers investigated was analyzed by incorporating statistical theories for unimolecular dissociation, specifically the Rice-Ramsperger-Kassel-Marcus (RRKM) treatment into eq S1 as described elsewhere.[7,8] Incorporation of lifetime effects into eq S1 requires sets of ro-vibrational frequencies appropriate for the energized complexes and the transition states (TSs) leading to dissociation. In our analysis, we assume that the TSs are loose and product-like because the interactions between the neutral and protonated nucleobases are largely electrostatic. The best model for the TS of such electrostatically bound complexes is a loose phase space limit (PSL) model located at the centrifugal barrier for the interaction between the neutral, 5*x*C, and protonated nucleobases, H^+(5*x*C), as described in detailed previously.[8] The parameters appropriate for the PSL TS are the frequencies and rotational constants of the 5*x*C and H^+(5*x*C) products, which are given in Table S1 and S2 of the Supporting Information.

The model represented by eq S1 is expected to be appropriate for translationally driven reactions[9] and has been found to reproduce CID cross sections well.[10-14] The model of eq S1 is convoluted with the kinetic and internal energy distributions of both the reactant (5*x*C)H^+(5*x*C) complex and neutral Xe atom, and a nonlinear least-squares analysis of the data is performed to give optimized values for the parameters, σ_0, E_0, and n. The error associated with the measurement of E_0 is estimated from the range of threshold values determined from the zero-pressure-extrapolated data sets, variations associated with uncertainties in the vibrational frequencies (± 10% scaling as discussed above), and the error in the absolute energy scale, 0.05 eV (Lab). For analyses that include the RRKM lifetime analysis, the uncertainties in the reported E_0(PSL) values also include the effects of increasing and decreasing the assumed time available for dissociation (~ 10^{-4} s) by a factor of two.

The internal energy of the reactant proton-bound homodimer, E_i, is explicitly included in eq S1. All energy available is treated statistically because the internal energy of the reactants is redistributed throughout the accessible ro-vibrational energy states of the reactant proton-bound homodimer upon collision with Xe.

Conversion from 0 to 298 K. To allow comparison to commonly employed experimental conditions, the 0 K BPEs determined here are converted to 298 K bond enthalpies and free energies. The enthalpy and entropy conversions are calculated using standard formulas (assuming harmonic oscillator and rigid rotor models) and the vibrational and rotational constants determined for the B3LYP/6-31G* optimized geometries, which are given in Tables S3 and S4 of the Supporting Information. Table S5 lists 0 and 298 K enthalpy, free energy, and enthalpic and entropic corrections for all systems experimentally determined.

References

(1) Ervin, K. M.; Armentrout, P. B. Translational Energy Dependence of $Ar^+ + XY \rightarrow ArX^+ + Y$ (XY = H_2, D_2, HD) from Thermal to 30 eV c.m. *J. Chem. Phys.* **1985**, *83*, 166–189.
(2) Dalleska, N. F.; Honma, K.; Armentrout, P. B. Stepwise Solvation Enthalpies of Protonated Water Clusters: Collision-Induced Dissociation as an Alternative to Equilibrium Studies. *J. Am. Chem. Soc.* **1993**, *115*, 12125–12131.
(3) Muntean, F.; Armentrout, P. B. Guided Ion Beam Study of Collision-Induced Dissociation Dynamics: Integral and Differential Cross Sections. *J. Chem. Phys.* **2001**, *115*, 1213–1228
(4) Beyer, T. S.; Swinehart, D. S. Number of Multiply-Restricted Partitions [A1]. *Commun. ACM*, **1973**, *16*, 379.
(5) Stein, S. E.; Rabinovitch, B. S. Accurate Evaluation of Internal Energy Level Sums and Densities Including Anharmonic Oscillators and Hindered Rotors. *J. Chem. Phys.* **1973**, *58*, 2438–2445.
(6) Stein, S. E.; Rabinovitch, B. S. On the Use of Exact State Counting Methods in RRKM Rate Calculations. *Chem. Phys. Lett.* **1977**, *49*, 183–188.
(7) Khan, F. A.; Clemmer, D. E.; Schultz, R. H.; Armentrout, P. B. Sequential Bond Energies of $Cr(CO)_x^+$, x = 1–6. *J. Phys. Chem.* **1993**, *97*, 7978–7987.
(8) Rodgers, M. T.; Ervin, K. M.; Armentrout, P. B. Statistical Modeling of Collision-Induced Dissociation Thresholds. *J. Chem. Phys.* **1997**, *106*, 4499–4508.
(9) Chesnavich, W. J.; Bowers. M. T. Theory of Translationally Driven Reactions. *J. Phys. Chem.* **1979**, *83*, 900–905.
(10) Chen, Y.; Rodgers, M. T. Structural and Energetic Effects in the Molecular Recognition of Acetylated Amino Acids by 18-Crown-6. *J. Am. Soc. Mass. Spectrom.* **2012**, *23*, 2020–2030.
(11) Austin, C. A.; Chen, Y.; Rodgers, M. T. Alkali Metal Cation-Cyclen Complexes: Effects of Alkali Metal Cation Size on the Structure and Binding Energy. *Int. J. Mass Spectrom.* **2012**, *330*, 27–34.
(12) Armentrout, P. B.; Yang, B.; Rodgers, M. T. Metal Cation Dependence of Interactions with Amino Acids: Bond Energies of Rb^+ and Cs^+ to Met, Phe, Tyr, and Trp. *J. Phys. Chem. B,* **2013**, *117*, 3771–3781.
(13) Nose, H.; Chen, Y.; Rodgers, M. T. Energy-Resolved Collision-Induced Dissociation Studies of 1,10-Phenanthroline Complexes of the Late First-Row Divalent Transition-Metal Cations: Determination of the Third Sequential Binding Energies. *J. Phys. Chem. A,* **2013**, *117*, 4316–4330.
(14) Nose, H.; Rodgers, M. T. Energy-Resolved Collision-Induced Dissociation Studies of 2,2'-Bipyridine Complexes of the Late First-Row Divalent Transition-Metal Cations: Determination of the Third Sequential Binding Energies. *Chem. Plus. Chem.* **2013**, *in press*, doi: 10.1002/cplu.201300156.

Table S1. Relative Energies at 0K in kJ/mol along the PESs for Dissociation of Proton-Bound (5*x*C)H^+(5*x*C) Homodimers Computed at Various Levels of Theory.

System	B3LYP		MP2(full)	
	Def2-TZVPPD	6-311+G(2d,2p)	Def2-TZVPPD	6-311+G(2d,2p)
(C)H^+(C)[a]	0.0	0.0	0.0	0.0
TS[a]	180.9	182.2	214.9	203.2
I$^+$•••**i**[b]	168.7	166.9	128.5	125.5
II$^+$•••**i**[b]	169.2	168.9	136.0	136.7
(5MeC)H^+(5MeC)[a]	0.0	0.0	0.0	0.0
TS[a]	184.3	184.7	219.0	206.3
I$^+$ + **i**[b]	169.1	167.7	137.1	125.9
II$^+$ + **i**[b]	173.3	173.4	140.4	141.0
(5FC)H^+(5FC)[a]	0.0	0.0	0.0	0.0
TS[a]	174.7	176.0	206.6	194.4
I$^+$ + **i**[b]	156.1	153.3	124.9	111.5
II$^+$ + **i**[b]	167.2	165.7	135.3	134.0
(5BrC)H^+(5BrC)[a]	0.0	0.0	0.0	0.0
TS[a]	173.8	174.7	202.1	192.4
I$^+$ + **i**[b]	156.5	152.3	119.8	111.4
II$^+$ + **i**[b]	162.8	161.5	126.1	127.6
(5IC)H^+(5IC)[a]	0.0	0.0	0.0	0.0
TS[a]	174.8	175.6	206.3	192.4
I$^+$ + **i**[b]	157.9	154.6	115.6	111.4
II$^+$ + **i**[b]	162.8	161.1	126.1	127.0

[a] Including ZPE corrections. [b]. Including ZPE and BSSE corrections

Table S2. Fitting Parameters of Equation 1, Threshold Dissociation Energies at 0 K, and Entropies of Activation at 1000 K of Proton-Bound (5*x*C)H^+(5*x*C) Homodimers[a]

x	σ[b]	n	E_0[c] (eV)	E_0(PSL)[b] (eV)	Kinetic Shift (eV)	$\Delta S^{\dagger}$ (PSL)[b] (J mol^{-1} K^{-1})
H	15.6 (2.5)	1.3 (0.16)	2.12 (0.05)	1.76 (0.04)	0.36	95 (4)
Me	22.3 (0.6)	0.9 (0.11)	2.49 (0.06)	1.84 (0.06)	0.65	94 (4)
F	154 (4.3)	1.0 (0.06)	2.06 (0.05)	1.69 (0.06)	0.37	98 (4)
Br	253 (23)	1.0 (0.12)	2.15 (0.06)	1.75 (0.05)	0.40	107 (4)
I	74.9 (5.7)	1.2 (0.06)	2.13 (0.07)	1.69 (0.05)	0.44	96 (6)

[a] Present results, uncertainties are listed in parentheses. [b] Average values for loose PSL TS. [c] No RRKM analysis.

Table S3. Vibrational Frequencies and Average Vibrational Energies of the Neutral, Protonated, and Proton-Bound Homodimers of Cytosine and 5-Substituted Cytosines.[a]

System	E_{int}, eV[b]	Frequencies[a]
$(C)H^+(C)$	0.35 (0.03)	41, 44, 98, 108, 130, 168, 177, 184, 192, 207, 386, 398, 406, 413, 440, 527, 533, 547, 550, 560, 568, 586, 628,631, 688, 707, 730, 737, 754, 774,778, 781, 787, 898, 956, 959, 967, 972, 992, 1004, 1029, 1103, 1110, 1131, 1140, 1219, 1224, 1267, 1288, 1371, 1389, 1440, 1465, 1496, 1517, 1542, 1554, 1629, 1655, 1657, 1689, 1715, 1729, 1809, 2700, 2934, 3178, 3185, 3191, 3201, 3404, 3534, 3539, 3571, 3611
$(5MeC)H^+(5MeC)$	0.44 (0.04)	29, 47, 88, 100, 116, 118, 124, 167, 177, 187, 191, 210, 291, 297, 301, 318, 393, 408, 410, 413, 440, 471, 484, 548, 555, 566, 584, 596, 625, 628, 716, 725, 733, 740, 741, 752, 754, 788, 797, 901, 811, 927, 958, 975, 1010, 1012, 1023, 1060, 1061, 1124, 1126, 1188, 1197, 1216, 1221, 1274, 1302, 1352, 1358, 1421, 1422, 1429, 1454, 1480, 1482, 1488, 1492, 1500, 1515, 1531, 1546, 1638, 1657, 1666, 1694, 1713, 1723, 1806, 2713, 2900, 2981, 3030, 3039, 3079, 3087, 3173, 3178, 3394, 3537, 3540, 3580, 3621
$(5FC)H^+(5FC)$	0.40 (0.04)	31, 48, 92, 99, 112, 125, 133, 165, 182, 209, 308, 321, 349, 350, 392, 396, 398, 413, 469, 483 (2), 539, 558, 591, 606, 611, 614, 615, 695, 705, 716, 728, 745, 760, 775, 795, 803, 890, 891, 908, 955, 972, 1026, 1115, 1119, 1182, 1186, 1240, 1243, 1302, 1303, 1338, 1342, 1430, 1454, 1504, 1534, 1546, 1560, 1642, 1660, 1674, 1705, 1712, 1730, 1807, 2665, 2923, 3196, 3197, 3399, 3535, 3538, 3558, 3603
$(5BrC)H^+(5BrC)$	0.43 (0.03)	19, 46, 73, 75, 82, 106, 110, 137, 180, 207, 222, 249, 281, 286, 289, 302, 404, 407, 413, 421, 499, 538, 558, 578, 591, 605, 627, 629, 631, 647, 712, 730, 735, 742, 752, 775, 786, 897, 827, 938, 957, 974, 1017, 1052, 1066, 1128 (2), 1194, 1197, 1263, 1292, 1324, 1331, 1424, 1451, 1496, 1515, 1520, 1535, 1625, 1637, 1639, 1683, 1708, 1722, 1808, 2715, 2922, 3190 (2), 3398, 3529, 3534, 3536, 3586
$(5IC)H^+(5IC)$	0.44 (0.04)	16, 47, 62, 67, 71, 97, 108, 132, 177, 200, 204, 220, 245, 256, 261, 268, 403, 405, 410, 421, 478, 538, 558, 571, 584, 586, 611, 631, 632, 635, 716, 720, 733, 738, 753, 774, 785, 905, 923, 934, 958, 975, 1016, 1029, 1044, 1122, 1127, 1195, 1197, 1265, 1296, 1326, 1332, 1421, 1449, 1493, 1508, 1515, 1529, 1614, 1630, 1637, 1684, 1710, 1721, 1810, 2728, 2914, 3191, 3192, 3394, 3529, 3534, 3536, 3584
C	0.15 (0.02)	136, 200, 318, 352, 386, 515, 523, 538, 566, 618, 718, 746, 755, 756, 908, 936, 971, 1082, 1112, 1120, 1239, 1340, 1425, 1492, 1550, 1627, 1674, 1784, 3153, 3176, 3519, 3546, 3639
5MeC	0.19 (0.02)	95, 193, 202, 269, 288, 339, 367, 394, 479, 530, 552, 578, 619, 724, 736, 753, 777, 901, 905, 1004, 1060, 1090, 1175, 1193, 1265, 1335, 1416, 1424, 1462, 1482, 1505, 1544, 1629, 1692, 1781, 2964, 3011, 3059, 3144, 3520, 3546, 3639
5FC	0.18 (0.02)	100, 195, 218, 284, 319, 372, 376, 474, 524, 540, 591, 593, 710, 740, 745, 777, 878, 900, 1065, 1162, 1191, 1270, 1320, 1419, 1502, 1555, 1621, 1705, 1783, 3179, 3536, 3548, 3660
5BrC	0.20 (0.02)	42, 84, 200 (2), 249, 276, 381, 387, 526, 560, 565, 613, 615, 730, 748, 757, 899, 918, 1019, 1072, 1182, 1245, 1310, 1414, 1475, 1629, 1617, 1666, 1787, 3172, 3537, 3542, 3662
5IC	0.20 (0.02)	68, 149, 175, 197, 223, 229, 376, 385, 525, 550, 556, 602, 621, 722, 752, 755, 902, 914, 999, 1081, 1185, 1247, 1312, 1412, 1469, 1520, 1616, 1658, 1789, 3170, 3530, 3540, 3652

Table S3. (continued) Vibrational Frequencies and Average Vibrational Energies of the Neutral, Protonated, and Proton-Bound Homodimers of Cytosine and 5-Substituted Cytosines.[a]

System	E_{int}, eV[b]	Frequencies[a]
H^+(C)	0.15 (0.02)	156, 182, 345, 404, 435, 486, 503, 525, 557, 649, 664, 710, 742, 768, 780, 941, 979, 996, 1062, 1120, 1181, 1237, 1376, 1391, 1473, 1556, 1590, 1651, 1688, 1867, 3185, 3203, 3493, 3508, 3516, 3611
H^+(5MeC)	0.19 (0.02)	113, 171, 185, 286, 293, 354, 404, 434, 462, 500, 528, 571, 647, 664, 725, 739, 778, 938, 939, 1008, 1062, 1066, 1171, 1213, 1231, 1348, 1378, 1427, 1463, 1483, 1492, 1550, 1587, 1656, 1685, 1864, 2989, 3043, 3092, 3177, 3494, 3512, 3519, 3617
H^+(5FC)	0.17 (0.02)	119, 176, 288, 332, 366, 386, 458, 461, 522, 540, 591, 632, 654, 696, 733, 758, 785, 929, 930, 1059, 1144, 1204, 1289, 1332, 1384, 1464, 1564, 1602, 1665, 1698, 1867, 3192, 3490, 3499, 3517, 3603
H^+(5BrC)	0.18 (0.02)	91, 172, 206, 270, 281, 370, 398, 457, 517, 548, 566, 619, 644, 660, 731, 740, 767, 938, 954, 1065, 1068, 1175, 1209, 1321, 1385, 1460, 1541, 1578, 1625, 1683, 1866, 3186, 3478, 3492, 3512, 3592
H^+(5IC)	0.19 (0.02)	81, 166, 180, 233, 246, 366, 397, 451, 517, 518, 559, 601, 647, 660, 720, 742, 767, 941, 948, 1044, 1061, 1177, 1209, 1324, 1384, 1458, 1534, 1574, 1616, 1680, 1866, 3186, 3476, 3492, 3512, 3589

[a] Determined at the B3LYP/6-31G* level of theory and scaled by 0.9804. [b] Uncertainties are listed in parentheses.

Table S4. Rotational Constants of Ground State Proton-Bound (5*x*C)H^+(5*x*C) Homodimers and PSL TSs for CID. Determined at the B3LYP/ 6-31G* Level of Theory

System	Energized Molecule		Transition State	
	1D[a]	2D[b]	1D[c]	2D[c]
(C)H^+(C)	0.033	0.009	0.127, 0.129	0.053, 0.054
(5MeC)H^+(5MeC)	0.027	0.007	0.102, 0.104	0.038, 0.039
(5FC)H^+(5FC)	0.027	0.007	0.105, 0.106	0.038, 0.039
(5BrC)H^+(5BrC)	0.023	0.003	0.096, 0.097	0.019, 0.020
(5IC)H^+(5IC)	0.022	0.002	0.094, 0.095	0.015, 0.015

[a] Active external. [b] Inactive external. [c] Rotational constants of the transition state treated as free internal rotors.

Table S5. Enthalpies and Free Energies of Base Pairing of Proton-Bound Homodimers at 298 K in kJ/mol[a]

x	ΔH_0	ΔH_0[b]	$\Delta H_{298} - \Delta H_0$[b]	ΔH_{298}	ΔH_{298}[b]	$T\Delta S_{298}$[b]	ΔG_{298}	ΔG_{298}[b]
H	169.9 (4.6)	169.2	0.8 (0.7)	170.7 (4.7)	170.0	52.9 (1.4)	117.8 (4.9)	117.1
Me	177.4 (5.3)	173.3	0.5 (0.7)	177.9 (5.3)	173.8	52.7 (1.5)	125.2 (5.6)	121.1
F	162.7 (3.8)	167.2	1.1 (0.4)	163.8 (3.8)	168.3	54.3 (0.8)	109.5 (3.9)	114.0
Br	168.5 (4.9)	162.8	1.6 (0.7)	170.1 (4.9)	164.4	58.1 (1.4)	112.0 (5.1)	106.3
I	163.2 (4.7)	162.8	1.1 (0.7)	164.3 (4.8)	163.9	55.4 (1.4)	108.9 (5.0)	108.5

[a] Present results, uncertainties are listed in parentheses. [b] Density functional theory calculations at the B3LYP/def2-TZVPPD with frequencies scaled by 0.9804.

Figure Captions

Figure S1. Cross sections for collision-induced dissociation of the proton-bound (5*x*C)H^+(5*x*C) homodimers, where *x* = H, F, Br, I, and Me, with Xe as a function of collision energy in the center-of-mass frame (lower *x*-axis) and laboratory frame (upper *x*-axis), parts a–d, respectively. Data are shown for the Xe pressure of ~0.1 mTorr.

Figure S2. B3LYP/6-31G* optimized geometries of the low-energy tautomeric conformations of 5-iodocytosine, 5IC, protonated 5-iodocytosine, H^+(5IC), and proton bound (5IC)H^+(5IC) homodimers. Relative Gibbs free energies at 298 K calculated at the B3LYP/6-311+G(2d,2p) level of theory with ZPE corrections included.

Figure S3. B3LYP/def2-TZVPPD potential energy surfaces for adiabatic and diabatic dissociation of the ground-state **II$^+$•••I_3a** conformation of the (5xC)H^+(5xC) homodimer to produce the ground-state conformations of neutral, 5*x*C_**i**, and protonated, H^+(5*x*C)_**I**$^+$, products and ground-state conformations of neutral, 5*x*C_**i**, and excited conformation of protonated, H^+(5*x*C)_**II**$^+$, products, respectively, where *x* = H, F, Br, and I.

Figure S4. Zero pressure extrapolated cross sections for collision-induced dissociation of the proton-bound (5*x*C)H^+(5*x*C) homodimers, where *x* = H, F, Br, and I, with Xe in the threshold region as a function of kinetic energy in the center-of-mass frame (lower *x*-axis) and the laboratory frame (upper *x*-axis), parts a–d, respectively. The solid lines show the best fits to the data using the model of eq 1 convoluted over the neutral and ion kinetic and internal energy distributions. The dotted lines show the model cross sections in the absence of experimental kinetic energy broadening for reactants with an internal temperature of 0 K. The data and models are shown expanded by a factor of 10 and offset from zero in the insets.

Figure S5. TCID measured (5*x*C)H^+(5*x*C) BPEs at 0 K (in kJ/mol), where *x* = H, F, Br, I, and Me, plotted versus B3LYP/6-311+G(2d,2p), MP2(full)/6-311+G(2d,2p), and MP2(full)/def2-TZVPPD theoretical values in parts a through c, respectively. The solid circles (●) represent theoretical values that include BSSE corrections, whereas the open circles (○) represent values without BSSE corrections. The black solid diagonal line indicates the values for which calculated and measured dissociation energies are equal. The black dotted and dashed lines are offset from the central diagonal line by the MADs calculated at the indicated level of theory for theoretical values including and excluding BSSE corrections, respectively.

Figure S1.

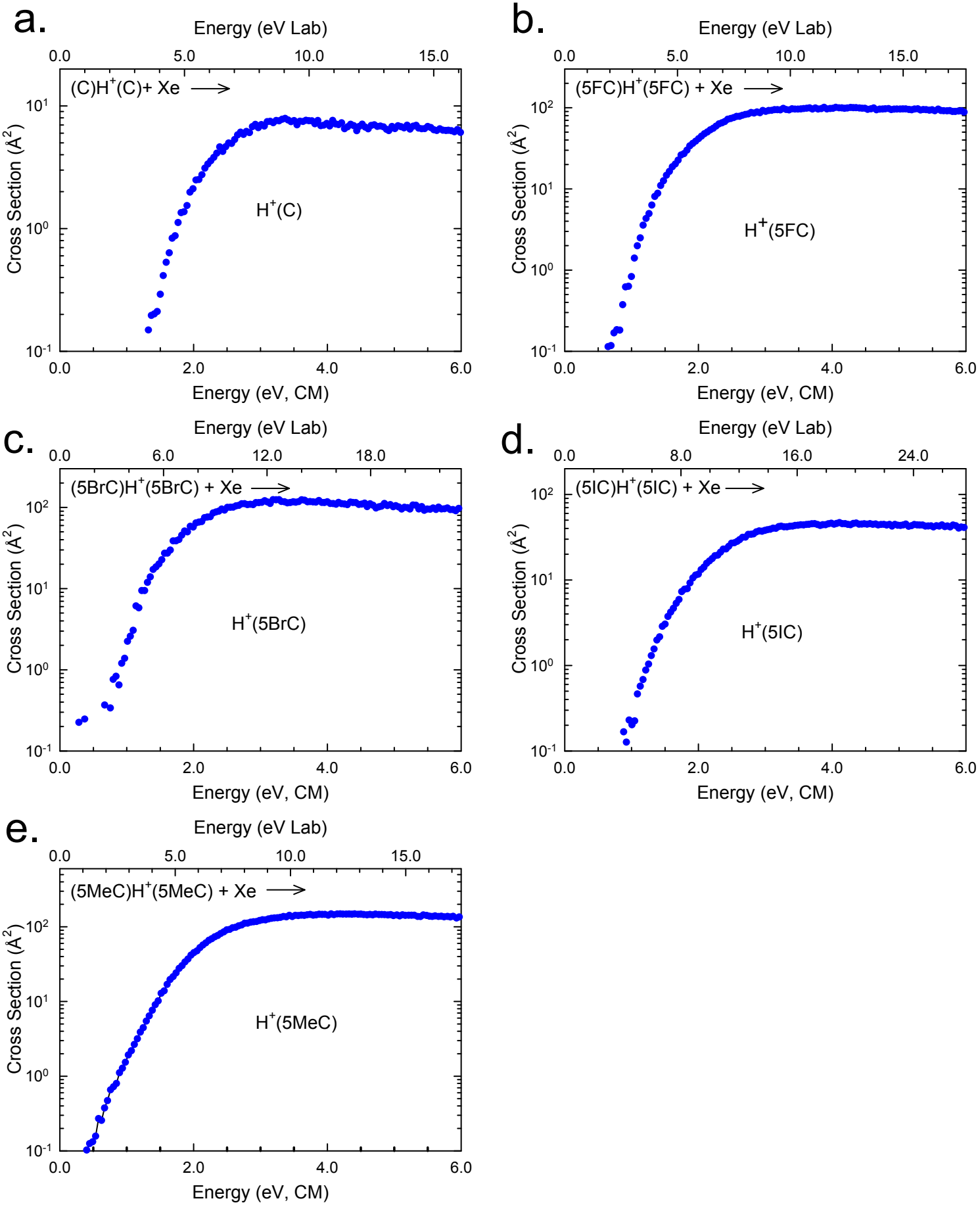
a.
Energy (eV Lab)
0.0
5.0
10.0
15.0
(C)H+(C)+ Xe
Cross Section (Å2)
H+(C)
0.0
2.0
4.0
6.0
Energy (eV, CM)
b.
Energy (eV Lab)
0.0
5.0
10.0
15.0
(5FC)H+(5FC) + Xe
Cross Section (Å2)
H+(5FC)
0.0
2.0
4.0
6.0
Energy (eV, CM)
c.
Energy (eV Lab)
0.0
6.0
12.0
18.0
(5BrC)H+(5BrC) + Xe
Cross Section (Å2)
H+(5BrC)
0.0
2.0
4.0
6.0
Energy (eV, CM)
d.
Energy (eV Lab)
0.0
8.0
16.0
24.0
(5IC)H+(5IC) + Xe
Cross Section (Å2)
H+(5IC)
0.0
2.0
4.0
6.0
Energy (eV, CM)
e.
Energy (eV Lab)
0.0
5.0
10.0
15.0
(5MeC)H+(5MeC) + Xe
Cross Section (Å2)
H+(5MeC)
0.0
2.0
4.0
6.0
Energy (eV, CM)

Figure S2.

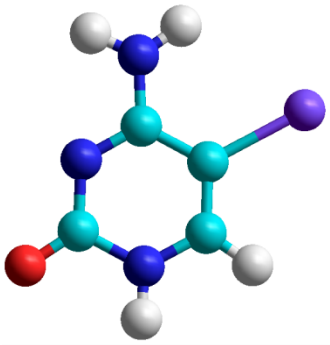

i

1.4 kJ/mol

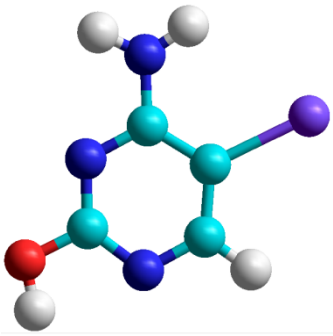

ii

0.0 kJ/mol

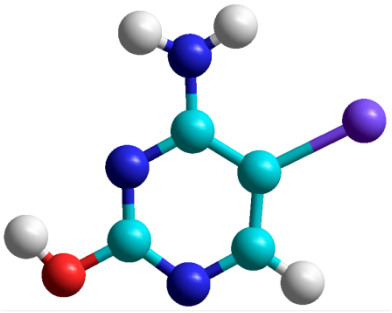

iii

2.8 kJ/mol

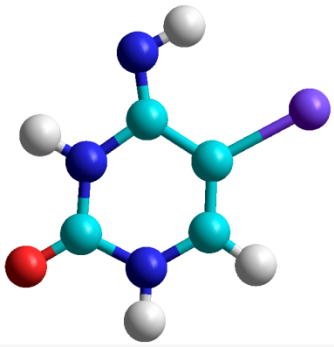

iv

14.1kJ/mol

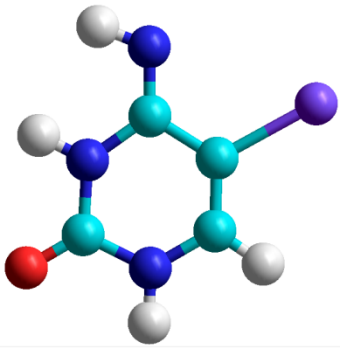

vi

23.5 kJ/mol

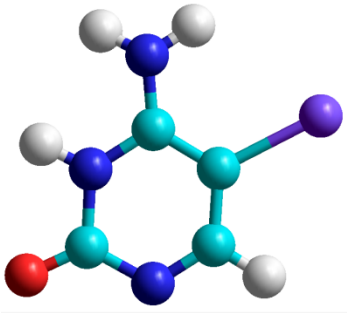

v

24.3 kJ/mol

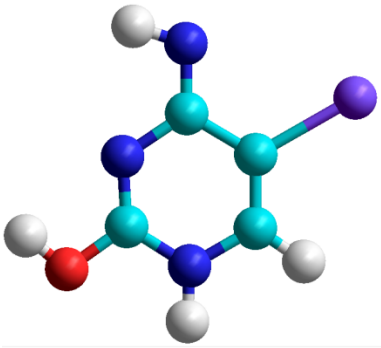

vii

68.7 kJ/mol

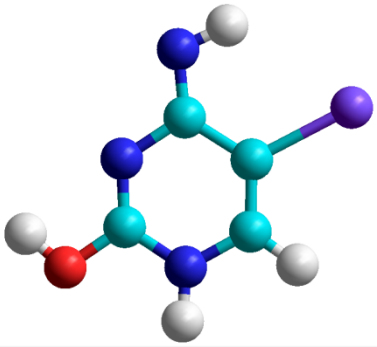

viii

77.4 kJ/mol

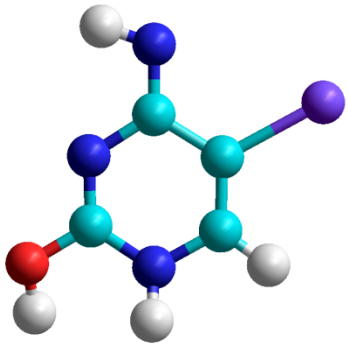

ix

98.6 kJ/mol

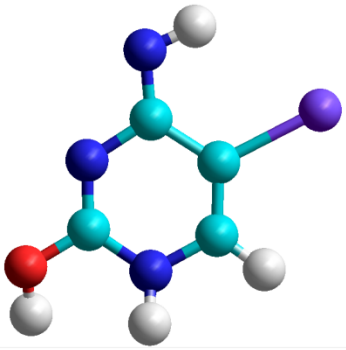

x

109.1 kJ/mol

5IC

Figure S2.

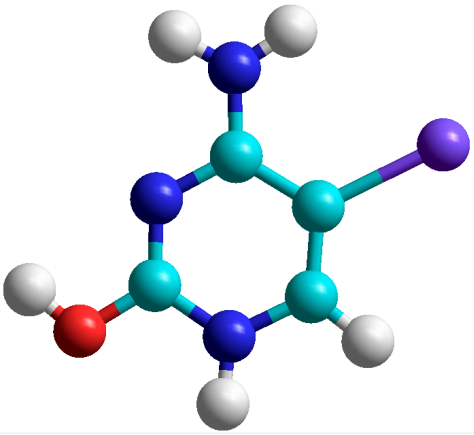

I^{+}

0.0 kJ/mol

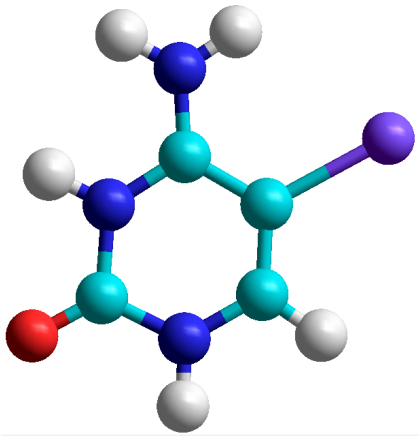

II^{+}

6.0 kJ/mol

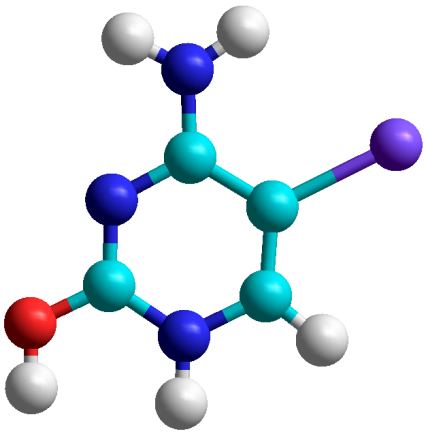

III^{+}

30.2 kJ/mol

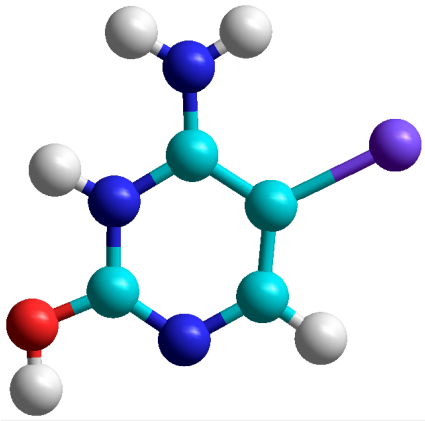

IV^{+}

34.0 kJ/mol

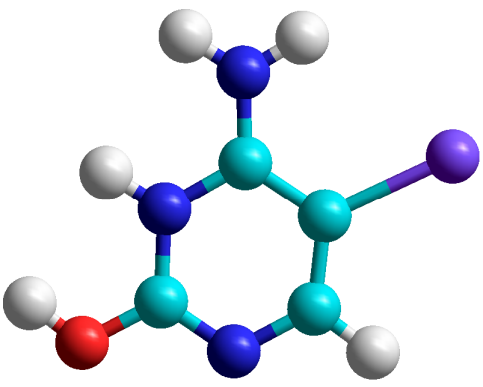

V^{+}

71.7 kJ/mol

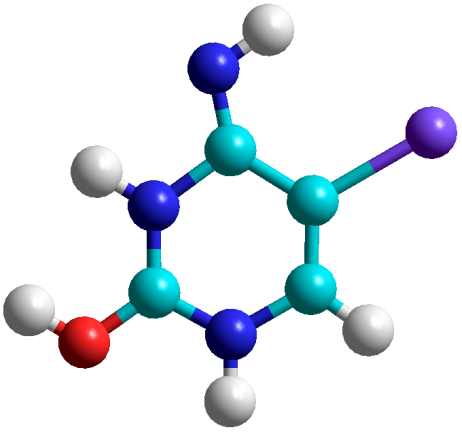

VI^{+}

115.7 kJ/mol

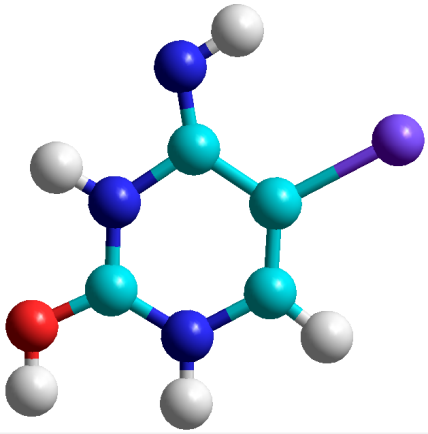

VII^{+}

119.6 kJ/mol

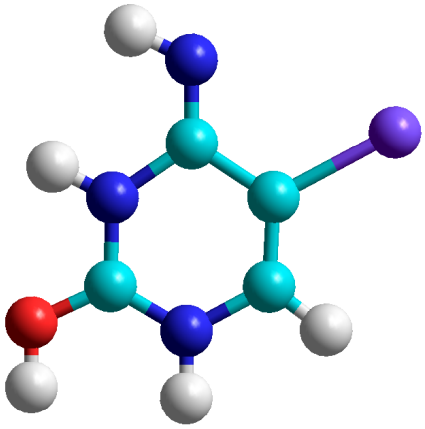

VIII^{+}

136.7 kJ/mol

H^{+}(5IC)

Figure S2.

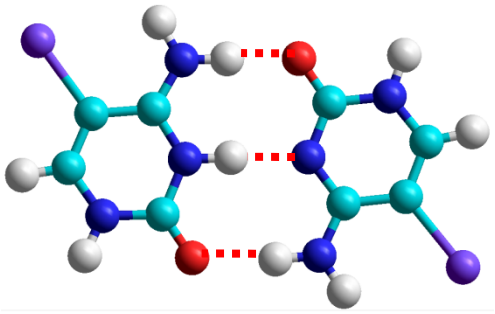

II$^+$•••i_3a
(N4H•O2, N3H•N3, O2•HN4)
0.0 kJ/mol

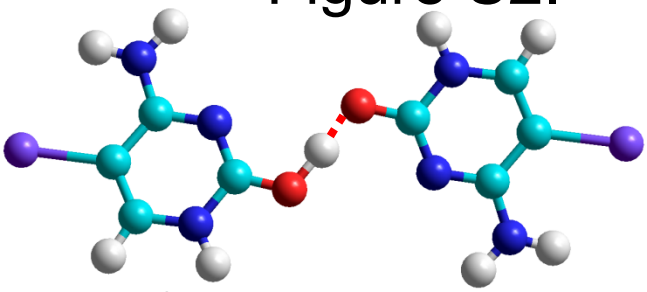

I$^+$•••i_1at (O2H•O2)
14.1 kJ/mol

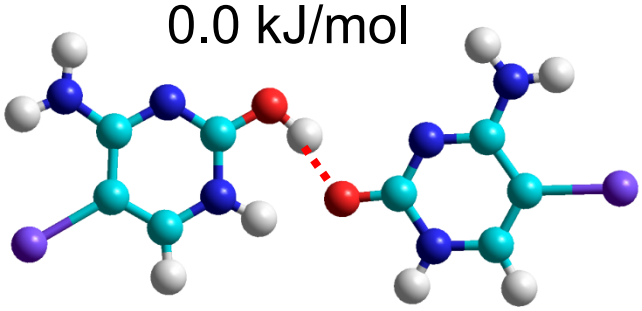

III$^+$••• i_1pt (O2H•O2)
24.5 kJ/mol

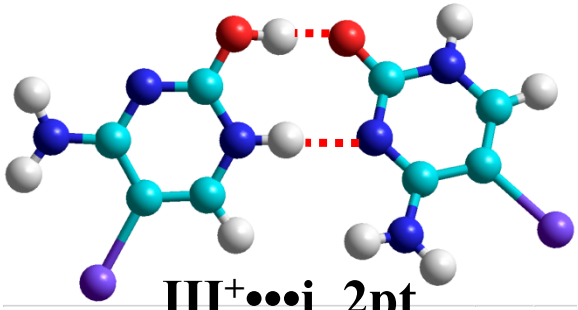

III$^+$•••i_2pt
(O2H•O2, N1H•N3)
31.1 kJ/mol

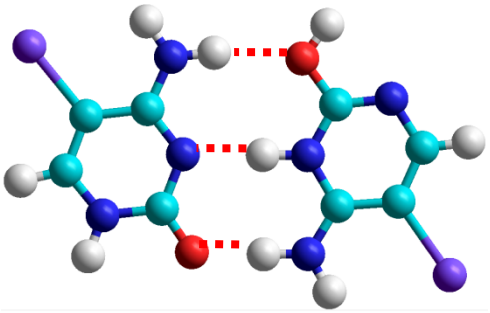

IV$^+$•••i_3a
(N4H•O2, N3H•N3, O2•HN4)
45.4 kJ/mol

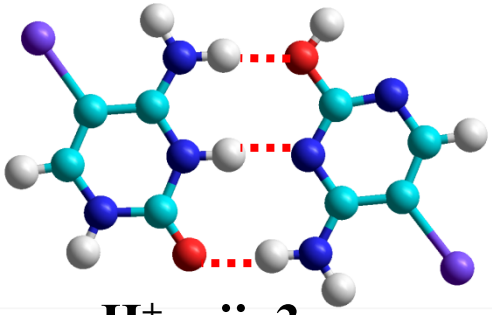

II$^+$•••ii_3a
(N4H•O2, N3H•N3, O2•HN4)
51.3 kJ/mol

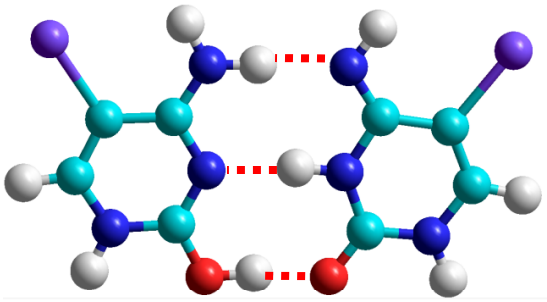

I$^+$•••iv_3p
(N4H•N4, N3•HN3, O2H•O2)
53.4 kJ/mol

(5IC)H$^+$(5IC)

Figure S2.

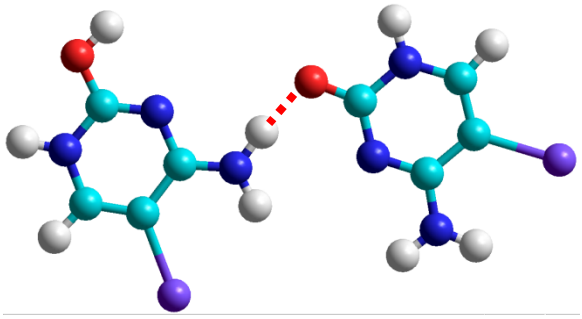

I^{+}•••**i_1pt** (N4H•O2)
55.2 kJ/mol

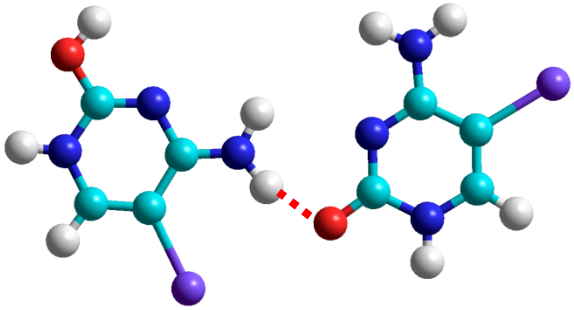

I^{+}•••**i_1at** (N4H•O2)
59.9 kJ/mol

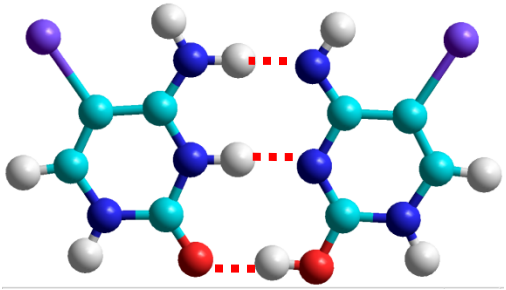

II^{+}•••**viii_3p**
(N4H•N4, N3H•N3, O2•HO2)
72.2 kJ/mol

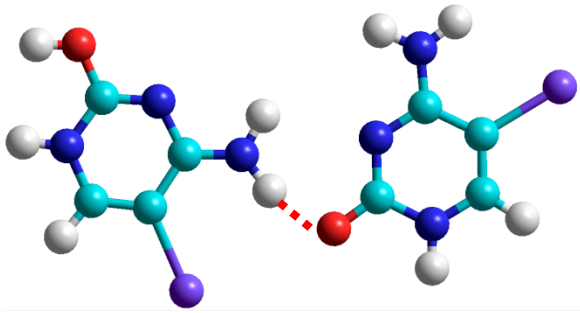

III^{+}•••**i_1at** (N4H•O2)
89.5 kJ/mol

(5IC)H^{+}(5IC)

Figure S3.

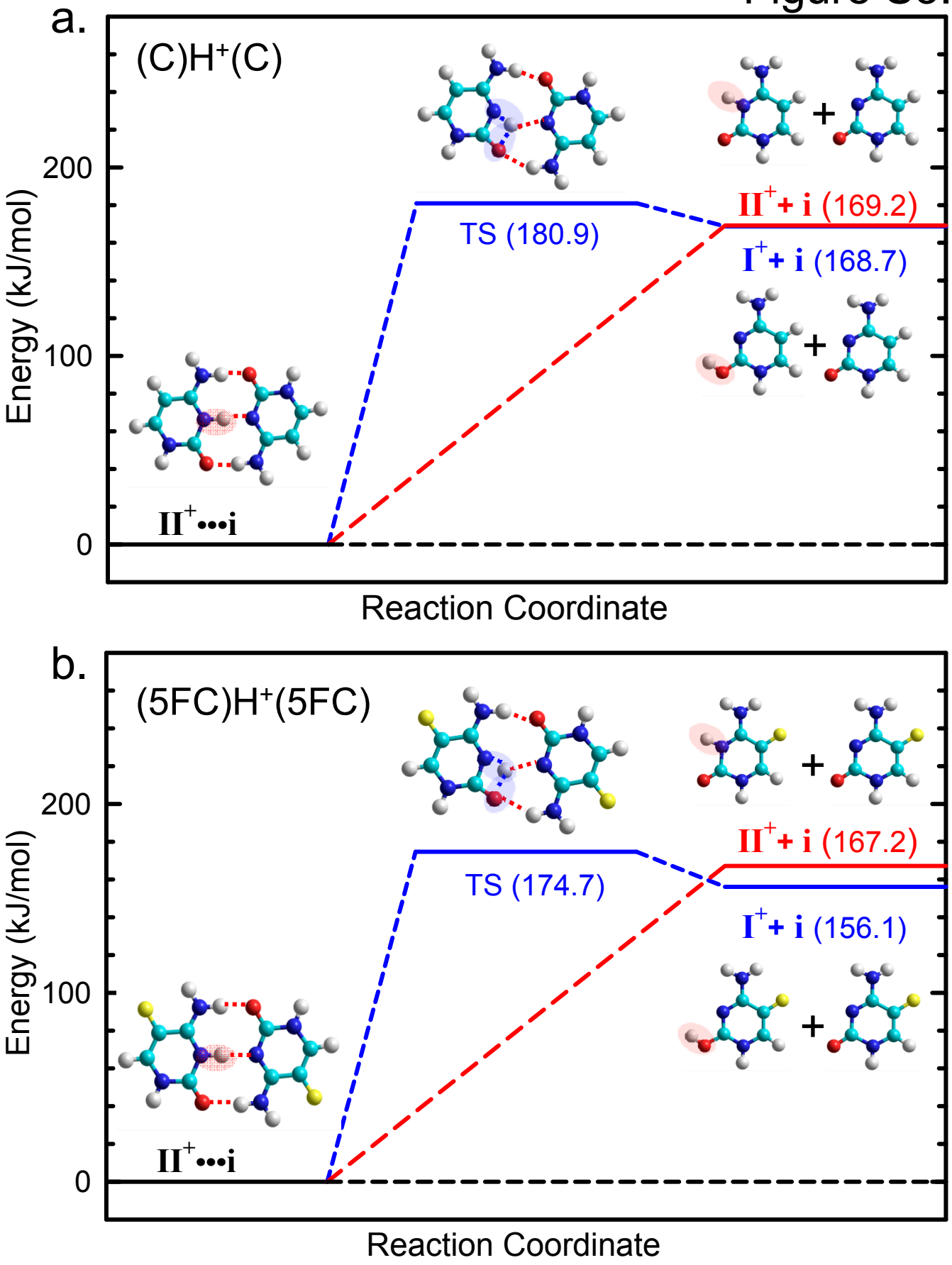
a.
(C)H+(C)
200
100
0
Energy (kJ/mol)
TS (180.9)
II+ + i (169.2)
I+ + i (168.7)
II+•••i
Reaction Coordinate
b.
(5FC)H+(5FC)
200
100
0
Energy (kJ/mol)
TS (174.7)
II+ + i (167.2)
I+ + i (156.1)
II+•••i
Reaction Coordinate

Figure S3.

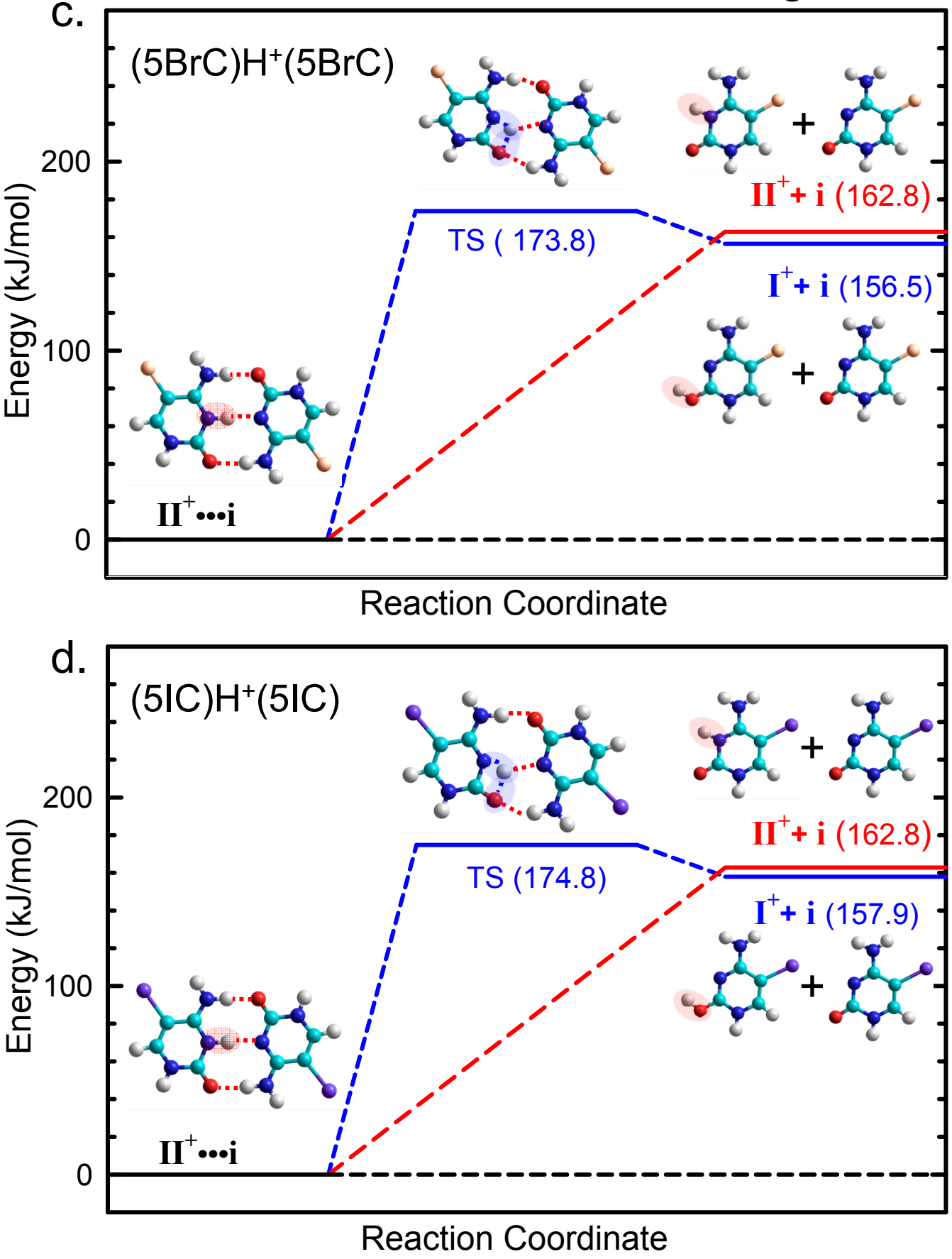
c.
(5BrC)H+(5BrC)
200
100
0
Energy (kJ/mol)
TS (173.8)
II+ + i (162.8)
I+ + i (156.5)
II+•••i
Reaction Coordinate
d.
(5IC)H+(5IC)
200
100
0
Energy (kJ/mol)
TS (174.8)
II+ + i (162.8)
I+ + i (157.9)
II+•••i
Reaction Coordinate

Figure S4.

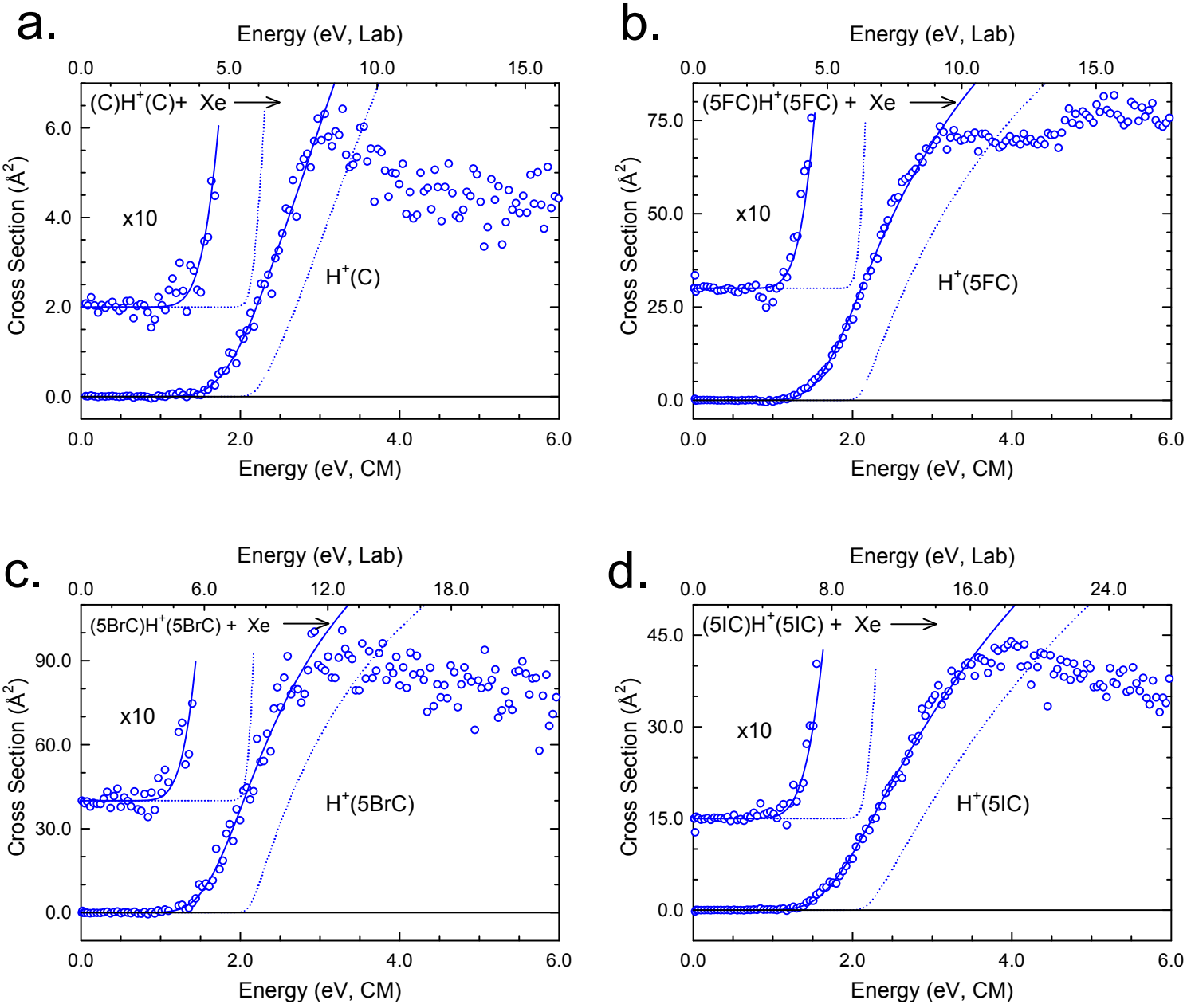
a.
Energy (eV, Lab)
(C)H+(C)+ Xe
x10
H+(C)
Cross Section (Å2)
Energy (eV, CM)
b.
Energy (eV, Lab)
(5FC)H+(5FC) + Xe
x10
H+(5FC)
Cross Section (Å2)
Energy (eV, CM)
c.
Energy (eV, Lab)
(5BrC)H+(5BrC) + Xe
x10
H+(5BrC)
Cross Section (Å2)
Energy (eV, CM)
d.
Energy (eV, Lab)
(5IC)H+(5IC) + Xe
x10
H+(5IC)
Cross Section (Å2)
Energy (eV, CM)

Figure S5.

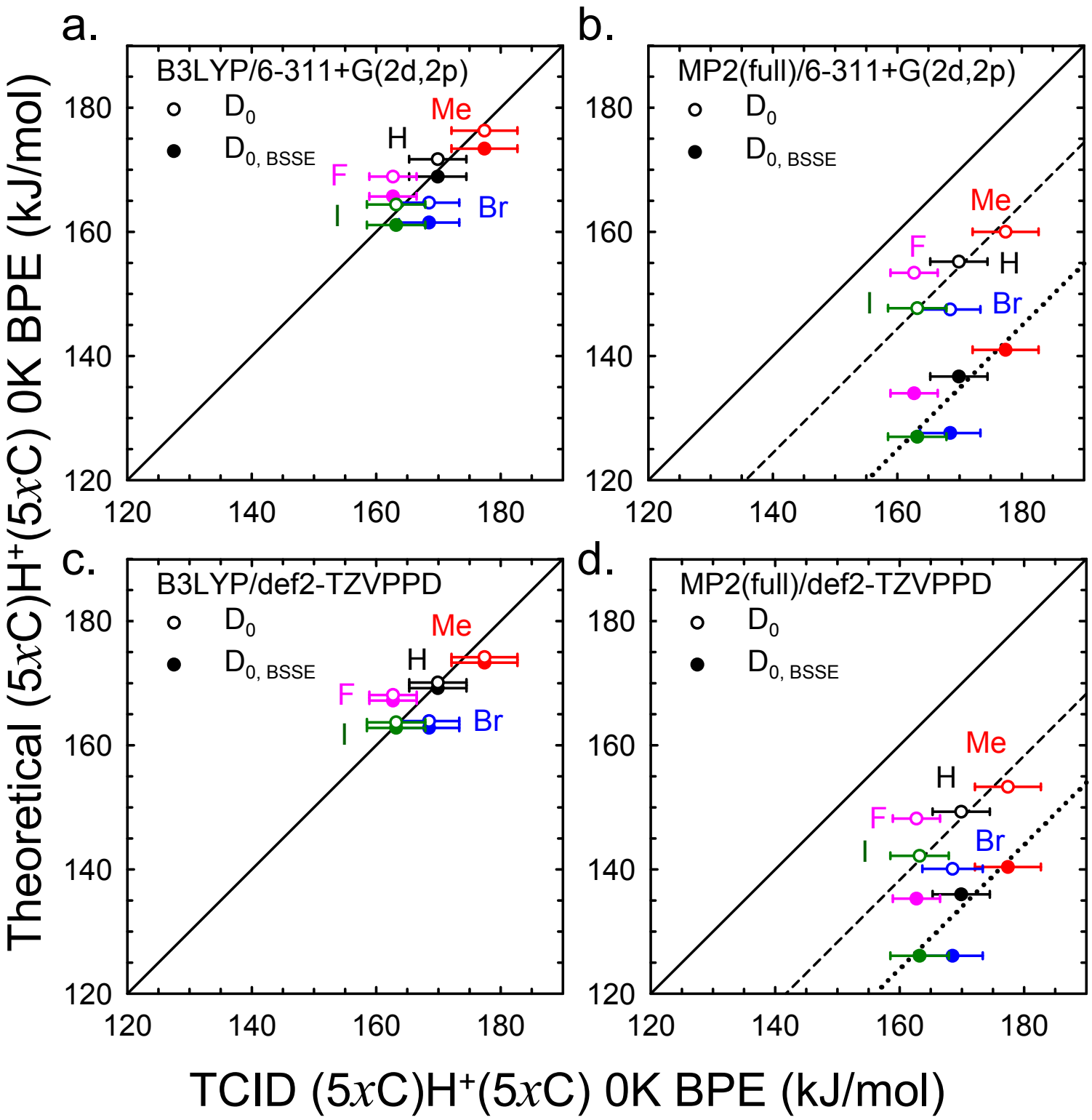
a.
B3LYP/6-311+G(2d,2p)
D0
D0, BSSE
Me
H
F
I
Br
b.
MP2(full)/6-311+G(2d,2p)
c.
B3LYP/def2-TZVPPD
d.
MP2(full)/def2-TZVPPD
120
140
160
180
Theoretical (5xC)H+(5xC) 0K BPE (kJ/mol)
TCID (5xC)H+(5xC) 0K BPE (kJ/mol)